From January 2009 *High Frequency Electronics*

An Improved Design Method For Stepped Line Microwave Filters with Broad Stop Bands

By Piotr Dyderski
Telecommunications Research Institute

The technique described here emphasizes proper setup of initial parameters before applying optimization in the well-known microwave EDA tools

The design problem for filters attenuating signals with frequencies outside the useful (pass) bands can be in many cases reduced to the problem of designing low pass or band-stop filters with sufficiently large bandwidths. It follows from the fact that some elements of complex electronic systems, as for example the radiating elements of antenna arrays, have the characteristics similar to those shown in Figure 1.

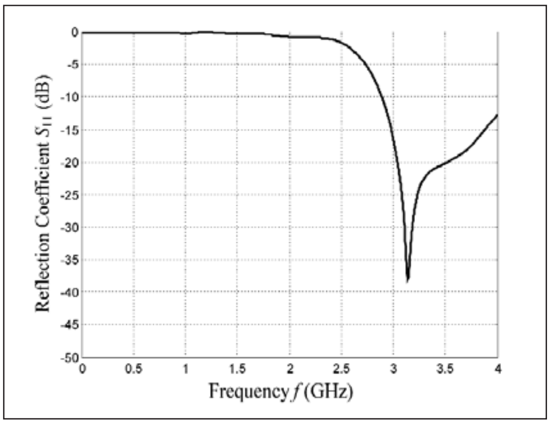

Figure 1 · Reflection coefficient S_{11} of a typical half-wave radiating element with operating frequency band centered at 3.5 GHz.

Among various possible implementations of band-stop filters, those implemented as a cascade connection of transmission line sections—the so-called stepped transmission line band-stop filters [1, 2]—are especially suitable for many applications. These filters are rather simple to manufacture, and their small cross-sections allow you to put them in place of specified sections of the transmission line. Among all analytical design methods, the most general is the one described in [1 - 4]. Its essential feature is the use of R-transformer as a prototype circuit together with the classical Darlington-Riblet method [1 - 5]. Unfortunately, the filters designed according to this last method may be difficult to manufacture in some cases because of the large spread of the characteristic impedances among the line sections. This follows from the fact that corresponding insertion loss function is formed by an appropriate choice of characteristic impedances of sections having equal electrical lengths. Consequently, for a fixed number of sections, the range of characteristic impedances increases when the requirements imposed on the relative stop band of the filter become more restrictive.

Therefore, the aim of this paper is to present the new approach that makes possible the design of band-stop filters with required insertion loss function (including filters with broad stop bands), which can be easily implemented in the prescribed technology. It can be obtained by limiting the range of characteristic impedances by application of optimization methods with constraints. Due to the fact that both characteristic impedances and electrical lengths of the sections are variables during the optimization process, this method belongs to the class of amplitude-phase methods.

The optimization process starts with an initial approximation found by means of an appropriate analytical method [1 - 4]. Naturally, the efficiency of the optimization strategy strongly depends on the quality of initial approximation. For example, analytical

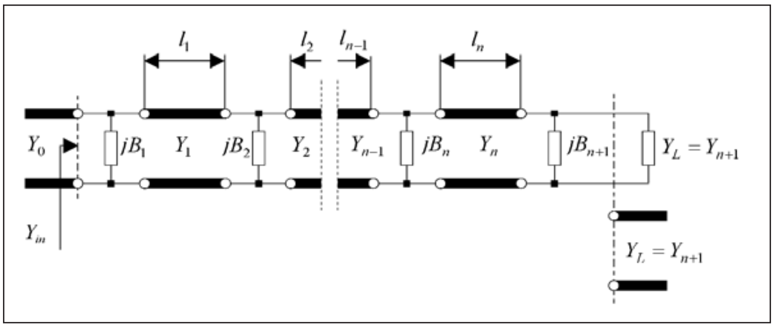

Figure 2 · Electrical scheme of the stepped transmission line band-stop filter.

formulas presented in [3] can be used to obtain filters with a maximum number of sections equal to 20, and their further enhancement would be extremely cumbersome. In the case of filters that require a large stop band, the initial approximation obtained in this way is unsuitable for the optimization process. For this reason, the original approach called "splining the insertion loss frequency response" has been proposed by the author.

In order to confirm the usefulness of the presented algorithm, three coaxial line filters have been designed, manufactured and tested. For one of the filters, the splining procedure was used for the insertion loss frequency response. Additionally, the influence of coaxial line step discontinuities has been investigated on the filter response.

Design Algorithm for Noncommensurate Band-Stop Filters

Let us consider the design of stepped transmission line band-stop filters with the electrical scheme shown in Figure 2.

The lumped-element susceptances B_i $(i = 1, 2, ..., n + 1)$ of the electrical scheme (see Fig. 2) represent discontinuities appearing in places of step changes of the line geometry. These susceptances can have capacitive ($B_i > 0$) or inductive ($B_i < 0$) character, depending on the kind of discontinuity. In general, the electrical equivalent scheme of the discontinuity is more complicated and the T or π two-port representation can be used [6], [7].

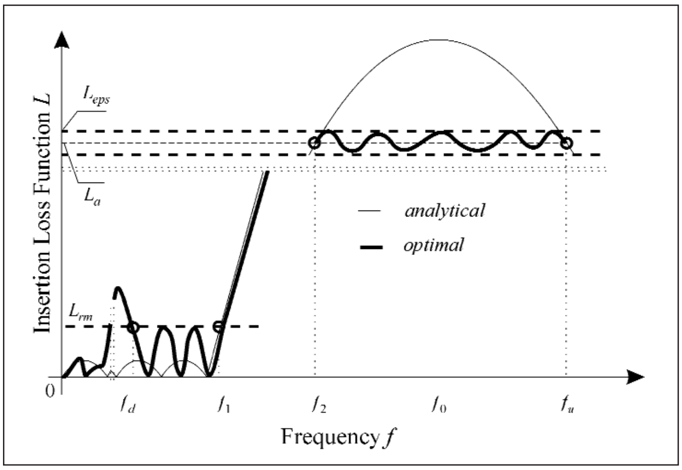

Figure 3 · Example of the insertion loss function *L* of the optimal and analytically designed filters.

It is assumed that optimal insertion loss function of the filter, similar to that shown in Figure 3, should be obtained as a result of the design process, which can be divided into two main stages. During the first stage, taking the R-transformer prototype circuit, the filter being initial approximation for the optimization process is found [1 - 3]. Depending on the assumed filter parameters (insertion loss response and range of characteristic impedances of its particular sections), this stage can be reduced to the design of a filter for which the R-transformer serves as the prototype. As an additional procedure, splining the insertion loss frequency response can be performed in this stage, as described later. The second stage of the design process is the optimization procedure for the filter structure.

Design of the Band-Stop Filters Based on the *R*-transformer Prototype Circuit

Let us assume that the output parameters defining insertion loss function in the prescribed frequency range are given (see Fig. 3), as well as the required characteristic impedance range of particular filter sections, determined by Z_{min} and Z_{max}. According to the relations given in [1 - 3], a minimum number of filter sections n_{min} can be found, for which the requirements imposed on the insertion loss response are satisfied. Next, for a given number of filter sections $n \geq n_{min}$, characteristic impedances of particular sections should be found [1 - 3]. It should be pointed out here that it is possible to design the filter satisfying all imposed requirements and containing smaller or greater number of sections $n \geq n_{min}$. Reduction of the number of sections leads to the larger spread of characteristic impedances. Initial approximation for the optimization process should be taken in the form of a filter with such number of sections n, that the range of characteristic impedances found analytically $\langle Z_{min\,A}; Z_{max\,A} \rangle$ is related to the required impedance range $\langle Z_{min}; Z_{max} \rangle$ by the following inequalities

$$\begin{cases} Z_{min\,A} \geq Z_{min} - 20, & (\Omega) \\ Z_{max\,A} \leq Z_{max} + 35, & (\Omega) \end{cases} \tag{1}$$

where the numbers 20 and 35 appearing in formula (1) determine the tolerance margin assumed by the author of this paper. In case, when these conditions cannot be satisfied, and when the initial approximation found analytically lies too far from the optimum, this approximation can be found using the procedure of splining the insertion loss frequency response, which is described in later.

Optimization Procedure for the Filter Structure

Let us assume that characteristic impedances and electrical lengths of particular filter sections have been found during the initial approximation stage of the design process. Input admittance $Y_{in} = G_{in} + jB_{in}$ of the filter shown in Figure 2 can be determined by multiple use of the standard impedance transformation equation, namely (see Fig. 4a)

$$Y_{in} = Y_k \frac{Y_L + jY_k tg(\beta_f l)}{Y_k + jY_L tg(\beta_f l)} \quad (2)$$

where $Y_{in} = G_{in} + jB_{in}$, $Y_L = G_L + jB_L$, $\beta_f = 2\pi/\lambda_f$, and λ_f is the line wavelength. For lossless TEM line section with dielectrical constant ε_r we have

$$\beta_f = \frac{2\pi}{\lambda_f} = \frac{2\pi f}{c\sqrt{\varepsilon_r}}.$$

Equation (2) written for the circuit of Figure 4b takes the following form

$$Y_{in} = Y_k \frac{Y_L + j\left[B + Y_k tg(\beta_f l)\right]}{Y_k - Btg(\beta_f l) + jY_L tg(\beta_f l)} \quad (3)$$

This complex equation can be easily separated into the real and imaginary parts, allowing all calculations to be made using operations on real numbers only. The input reflection coefficient Γ is related to the input admittance through the following simple formulas (see Fig. 2):

$$\Gamma(f) = \frac{Y_0 - Y_{in}(f)}{Y_0 + Y_{in}(f)} = \frac{\left[Y_0 - G_{in}(f)\right] - jB_{in}(f)}{\left[Y_0 + G_{in}(f)\right] + jB_{in}(f)}$$
$$\left|\Gamma(f)\right|^2 = \frac{\left[Y_0 - G_{in}(f)\right]^2 + B_{in}^2(f)}{\left[Y_0 + G_{in}(f)\right]^2 + B_{in}^2(f)} \quad (4)$$

The insertion loss function $L(f)$ of the filter is related to the reflection coefficient $\Gamma(f)$ as follows

$$L(f) = \frac{1}{\left|S_{21}(f)\right|} = \frac{1}{1 - \left|\Gamma(f)\right|^2} \quad (5)$$

where $S_{21}(f)$ is the coefficient of scattering matrix **S**.

In order to perform the optimization process (obtaining optimal insertion loss response, see Fig. 3) the following objective function should be applied

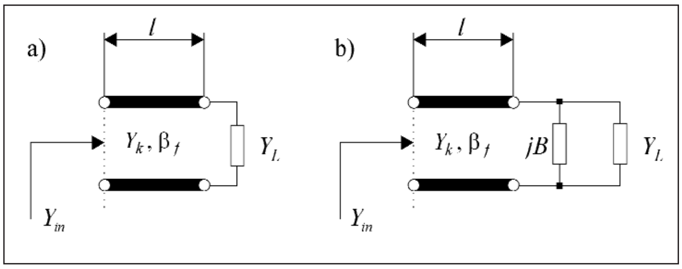

Figure 4 · Illustration of the impedance (admittance) transformation equation with (a) and without (b) the influence of discontinuities.

$$OF(f_i;\mathbf{p}) = \begin{cases} W(f_i)\cdot L(f_i;\mathbf{p}) & f_i \in \langle f_d; f_1 \rangle \\ W(f_i)\cdot \left|L(f_i;\mathbf{p}) - L_a\right| & f_i \in \langle f_2; f_u \rangle \end{cases} \quad (6)$$

where $W(f_i)$ is the weighting function

$$W(f_i) = \begin{cases} \dfrac{L_{eps} - L_a}{L_{rm}} & f_i \in \langle f_d; f_1 \rangle \\ 1 & f_i \in \langle f_2; f_u \rangle \end{cases} \quad (7)$$

Parameter L_a is the nominal value of insertion loss in the stop band, ($L_{eps} - L_a$) is the maximum loss deviation in the stop band, and L_{rm} is maximum reflection loss in the pass band (see Fig. 3). In the general case of amplitude-phase synthesis, the vector of parameters "**p**" (variables during the optimization process) is composed of $\mathbf{p} \equiv [Z_1,...,Z_n,l_1,...,l_n]$. The set of admissible solutions Φ determines the values of characteristic impedances and geometrical lengths of the sections

$$Z_{\min} \le Z_i \le Z_{\max}$$
$$l_i \ge l_{\min} \quad i \in [1:n] \quad (8)$$

and the requirements imposed on the range of characteristic impedances of particular sections are tightly involved with the line geometry.

The objective function $OF_p(f_i;\mathbf{p})$ satisfying the above requirements takes the form

$$OF_p(f_i;\mathbf{p}) = OF(f_i;\mathbf{p}) + P(\mathbf{p};t_1,t_2) \quad (9)$$

where $P(\mathbf{p}; t_1, t_2)$ is the penalty component defined as follows

$$P(\mathbf{p};t_1,t_2) = \exp\left[\sum_{j=1}^{n} t_1\left(Z_{\min} - Z_j\right)\right] +$$

$$+\exp\left[\sum_{j=1}^{n} t_1\left(Z_j - Z_{\max}\right)\right] + \exp\left[\sum_{j=1}^{n} t_2\left(l_{\min} - l_j\right)\right] \quad (10)$$

Positive weighting coefficients t_1, t_2 are gradually incremented during consecutive iterations. Finally, the optimization problem can be written as

$$\min_{\mathbf{p}\in\Phi} \max_{i\in[1:N]} OF_p\left(f_1;\mathbf{p}\right) \quad (11)$$

Problem (11) can be solved by means of the ε-steepest descent methods [8, 9]. The essence of these methods and their application to the stepped transmission line band-stop filter design was discussed extensively in [3, 10].

Application of the Optimization Procedure to the Band-Stop Filters Implemented with Coaxial Line

Let us consider the band-stop filter design using the coaxial line technology. (Experimental examples of these filters will be described in the next section.) Cross- and longitudinal-sections of the step change of coaxial line inner conductor diameter [11] are shown in Figures 5a and 5b, respectively. The equivalent circuit at reference plane T is shown in Figure 5c.

The following equality holds for the plane T of the step change of the line transversal dimensions [11]

$$\frac{Y_0'}{Y_0} = \frac{\ln\left(\dfrac{c}{a}\right)}{\ln\left(\dfrac{c}{b}\right)} \quad (12)$$

The normalized susceptance B/Y_0 can be calculated from the formulas given in [11]. For this purpose it is necessary to solve the following nonlinear equation

$$J_0(\chi)N_0\left(\frac{\chi c}{a}\right) - N_0(\chi)J_0\left(\frac{\chi c}{a}\right) = 0 \quad (13)$$

The first, nonvanishing root of this equation can be evaluated from the approximate relation [12, 13]

$$\chi_{01} \cong \sqrt{\frac{\pi^2}{(g-1)^2} - \frac{1}{(g+1)^2}} \quad (14)$$

where $g = c/a$ and $Z_m(g\chi) = J_m(g\chi)N_m(\chi) - N_m(g\chi)J_m(\chi)$ is the combination of Bessel-Neumann function of the order m.

The step changes of the coaxial line inner conductor diameter presented in Figure 6 are approximately equivalent. Equivalent circuit for the step change of outer conductor dimensions of the coaxial line is given in [11].

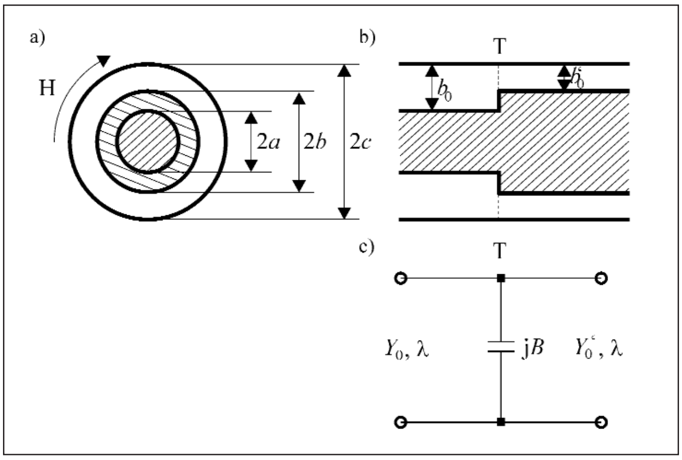

Figure 5 · Cross-section (a), longitudinal section (b) and equivalent circuit (c) of the step change of outer conductor diameter of the coaxial line.

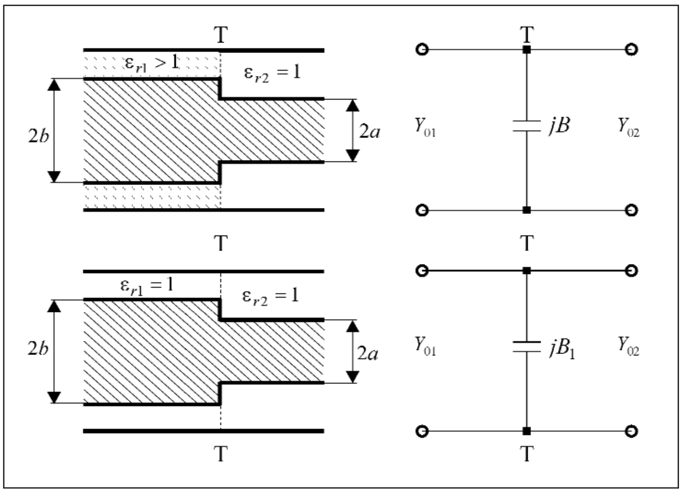

Figure 6 · Equivalent circuits for step dimension changes of coaxial line inner conductor ($B \cong B_1$).

Equivalent circuits of geometry changes for different kinds of lines can be found in many publications, as for example in [7].

It is recommended to perform the filter design first without taking into account the effect of discontinuities. Next for a chosen structure (layout of the dielectric supports) this process should be continued up to the end, using the method in which presence of discontinuities is assumed.

Procedure of Splining the Insertion Loss Frequency Response

Standard microwave band-stop filters incorporating commensurate sections of transmission lines have as a rule the periodically repeated stop bands, situated around the odd harmonics of frequency f_0, which is the center frequency of the first stop band. (This is strictly true for the TEM line. In case of the dispertion lines it refers to the wavelength λ, see for example [14].) It means that pass bands separate consecutive stop bands of the filter (see Fig. 7). (Similar situation of the pass bands repetition occurs in case of the band-pass filters [14].) The procedure of splining the insertion loss frequency response uses the property that in the pass band, where the reflection loss is small, input impedance of the filter is approximately equal to the terminal impedance $Z_{in} \approx Z_L$ ($Y_{in} \approx Y_L$), see Figure 2. It is then possible to connect together the filters having appropriate frequency shift of insertion loss functions, without introducing significant deformation of their characteristics [15]. The initial approximation obtained by use of the spline procedure has the characteristic impedance distribution, which is closer to the optimum and provides excess reduction of the insertion loss in the middle of the stop band (see Fig. 3).

Figure 7 illustrates periodicity of the insertion loss function of an analytically designed band-stop filter with commensurate sections having $\lambda_0/4$ length at the stop band center frequency f_0. The second filter of the cascade structure should be designed to have the central part of its stop band at $2f_0$, that is its stop band should be situated between the first and the second stop band of the first filter. Due to the finite slope of insertion loss responses, the stop band width of the second cascaded filter should be reduced in order to minimize the overlapping effect. It can be assumed that the insertion loss responses of cascaded filters should "intersect" in the middle of the nominal value of the loss assumed in the stop band (in dB scale), see Figure 8. Analogical procedures can be applied in case of greater number of cascaded filters (see Fig. 9).

Example of Application of the Splining Procedure for the Insertion Loss Frequency Responses in Order to Obtain Initial Approximation for the Optimization Process

Let us consider the design of band-stop filter with stopband frequency response described by means of the following parameters: f_d = 1.20 GHz, f_1 = 1.45 GHz, f_2 = 2.0 GHz, f_u = 12 GHz, and also S_{11} < –23 dB over the whole pass band and the minimum value of the reflection losses in the stop band equal to 20 dB (see Fig. 3). The admissible characteristic impedance range of particular filter sections is limited by Z_{min} = 25 Ω and Z_{max} = 90 Ω. The characteristic impedance range for the band-stop filter designed using R-transformer with 20 sections is given by $Z_{min\,A}$ = 10 Ω and $Z_{max\,A}$ = 240 Ω. As condition (1) is not satisfied, the procedure of splining the insertion loss frequency response should be applied in order to obtain better initial approximation for the optimization process.

Let us now assume that the band-stop filter composed of two filters (having 18 and 14 sections, respectively) was designed on the base of the R-transformer prototype with nominal loss 25 dB in the stop band. The insertion loss functions of the cascaded filters are presented in Figure 8a. Figure 8b shows the insertion loss of two filters in cascade. Significantly higher loss excess in the stop band of the first cascaded filter is the consequence of its much larger relative stop bandwidth. The range of characteristic impedances of the particular sections of the initial approximation is 20.9 Ω ≤ Z_i ≤

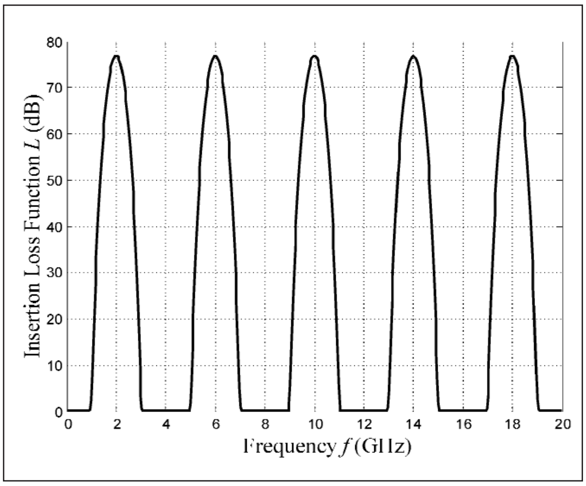

Figure 7 · Illustration of periodical repetition of stop bands for analytically designed stepped transmission line band-stop filter with commensurate sections.

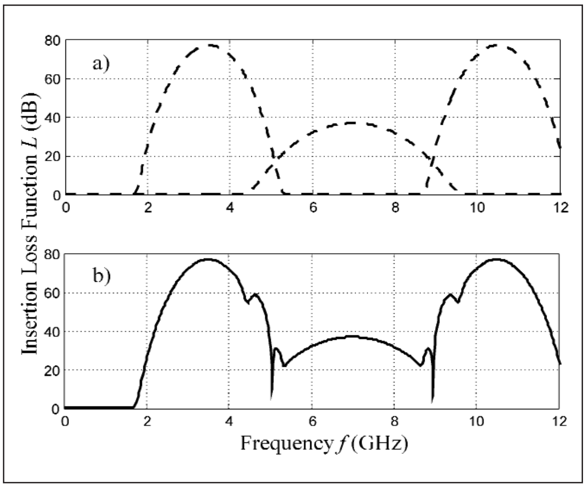

Figure 8 · Insertion loss functions of two cascaded filters (a) and cascade connection of the filters (b).

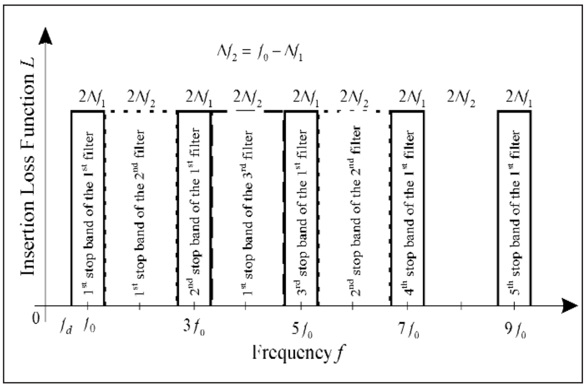

Figure 9 · Stop bands of three cascaded filters.

119.4 Ω. The filter designed in this manner satisfies condition (1) and can be used as a good approximation for the next optimization stage.

Experimental Results

In order to confirm the usefulness of the design method presented in this paper, three coaxial band-stop filters have been constructed and tested. Two of them, designated Filter I and Filter II, were designed assuming presence of discontinuities appearing in places where there is a step change of line geometry. The third filter, Filter III, was designed by means of the splining procedure, applied to the insertion loss frequency responses, without influence of discontinuities. Characteristics of the filters obtained experimentally were compared with theoretical curves, and the influence of discontinuities on the characteristics of the designed filters was considered.

Filter I

The first filter was designed assuming the following parameters: f_d = 3.1 GHz, f_1 = 3.6 GHz, f_2 = 4.55 GHz and f_u = 10 GHz (see Fig. 3) with the admissible characteristic impedance range given by Z_{min} = 20 Ω and Z_{max} = 100 Ω. It was assumed that S_{11} < –23 dB in the pass band with the loss in the stop at least 40 dB. The filter was implemented in the coaxial line technology, with the diameter of the outer conductor equal to 10 mm, and terminated with 50 Ω type N connectors.

During the first design stage, parameters of the band-stop filter having 20-sections were evaluated using R-transformer prototype. Characteristic impedances of this initial approximation are limited to the range determined by $Z_{min\,A}$ = 22.7 Ω and $Z_{max\,A}$ = 110.2 Ω, satisfying condition (1). In the next stage, the filter was optimized, taking into account the influence of discontinuities. During the optimization process, the characteristic impedance of the last

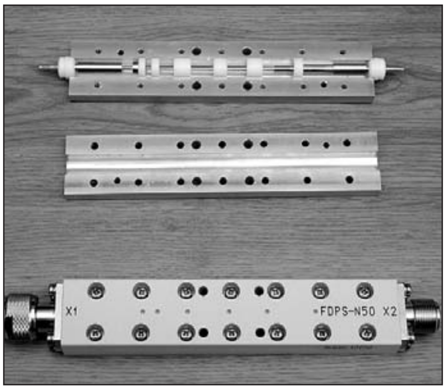

Figure 10 · Construction outline of Filter I.

section resulted in a value of 50 Ω. Thus, the filter is composed of 19 sections. Parameters of the filter obtained after the optimization process are given in Table 1 and construction of the filter is shown in Figure 10.

Figure 11 and Figure 12 show the experimental and theoretical S_{11} and S_{21} responses of the filter. Theoretical characteristics were computed assuming the influence of discontinuities, according to the model introduced in this paper. It should be pointed out that there is a very good agreement between these curves in the whole analyzed frequency range. In spite of the potential for higher, parasitic modes, their influence on filter responses was not observed.

For evaluation of the influence of discontinuities on the filter response, experimental and theoretical curves

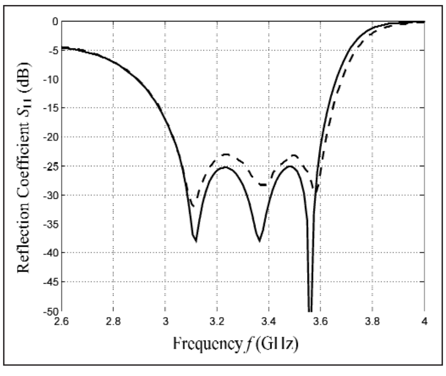

Figure 11 · Theoretical (solid line) and experimental (dashed line) S_{11} responses of Filter I.

Section No. i	Z_{0i} (Ω)	Inner conductor diameter d_i (mm)	Dielectric constant ε_r	Section length l_i (mm)
1	37.1	5.39	1	7.39
2	38.2	5.29	1	13.74
3	91.9	2.16	1	5.41
4	31.3	5.93	1	2.81
5	20.0	6.22	2.06	3.04
6	100.0	1.89	1	3.06
7	20.0	6.22	2.06	3.60
8	100.0	1.89	1	6.92
9	20.0	6.22	2.06	7.98
10	100.0	1.89	1	10.88
11	20.0	6.22	2.06	6.52
12	97.8	1.96	1	9.46
13	20.0	6.22	2.06	7.27
14	100.0	1.89	1	6.09
15	67.2	3.27	1	9.43
16	20.0	6.22	2.06	4.35
17	52.2	4.19	1	11.79
18	48.2	4.48	1	3.57
19	30.8	5.98	1	15.59
			$\sum l_i$ –	138.90

Table 1 · Electrical and construction parameters of Filter I.

were compared (with no discontinuity influence taken into account), see Figure 13. It was observed that there is some degradation of the resulting theoretical S_{11} response in the pass band. It was also found that theoretical responses are shifted towards higher frequencies, and the theoreti-

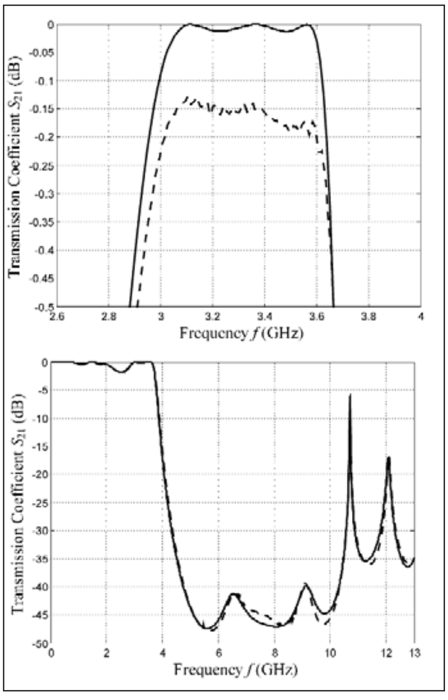

Figure 12 · Theoretical (solid line) and experimental (dashed line) S_{21} responses of Filter I.

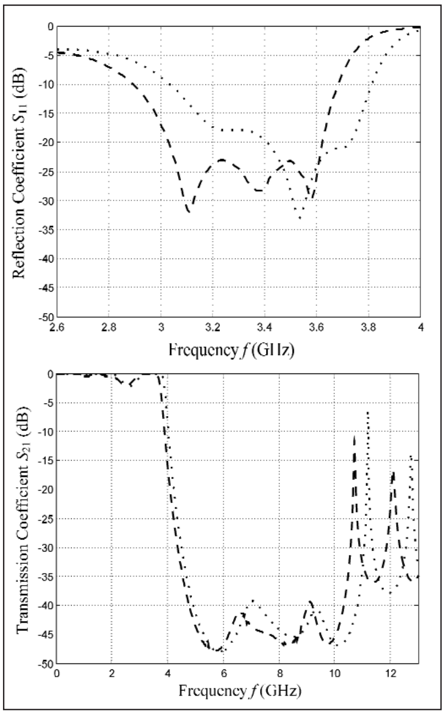

Figure 13 · Comparison of experimental (dashed line) and theoretical (dotted line) S_{11} and S_{21} responses of Filter I obtained assuming the lack of discontinuities.

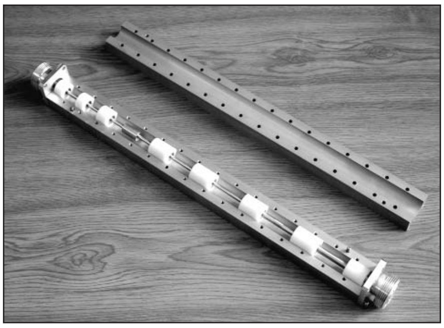

Figure 14 · Construction outline of Filter II.

Section No. i	Z_{0i} (Ω)	Inner conductor diameter d_i (mm)	Dielectric constant ε_r	Section length l_i (mm)
1	27.0	8.42	2.03	9.57
2	81.6	4.10	1	15.37
3	26.0	8.63	2.03	9.23
4	90.0	3.57	1	15.42
5	25.0	8.83	2.03	11.91
6	87.0	3.75	1	14.58
7	34.7	8.97	1	15.91
8	90.0	3.57	1	16.32
9	25.0	8.83	2.03	19.49
10	87.1	3.74	1	24.62
11	26.0	8.63	2.03	20.72
12	86.3	3.79	1	30.71
13	26.8	8.47	2.03	19.71
14	70.2	4.97	1	30.86
15	26.9	8.44	2.03	22.40
16	63.2	5.58	1	26.98
17	34.0	7.13	2.03	17.41
			$\sum l_i =$	321.21

Table 2 · Electrical and construction parameters of Filter II.

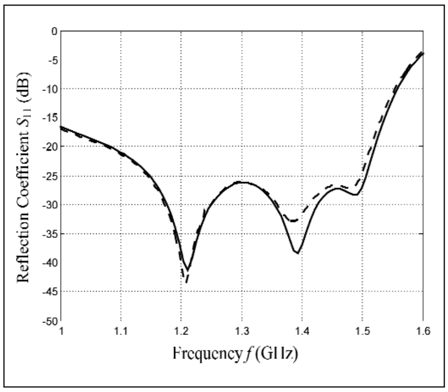

Figure 15 · Theoretical (solid line) and experimental (dashed line) S_{11} responses of Filter II.

cal stop band is wider than the experimental one. This means that the filter designed primarily without considering the discontinuities should be shortened (each section) by 1 or 2 percent, in order to obtain a response close to the theoretical curves.

Filter II

The second filter was designed to meet the following requirements: f_d = 1.15 GHz, f_1 = 1.5 GHz, f_2 = 2.1 GHz and f_u = 6 GHz (see Fig. 3) with the characteristic impedance range of particular sections given by Z_{min} = 25 Ω and Z_{max} = 90 Ω. It was assumed that S_{11} < –23 dB in the pass band with the stop band loss at least 30 dB. The filter was implemented in coaxial line technology, with the diameter of outer conductor equal to 16 mm, and terminated with standard 7/16 connectors (VSWR < 1.01 in the pass band and VSWR < 1.15 in the stop band was obtained).

In the first design stage, parameters of a band-stop filter having 18-sections and designed on the basis of the R-transformer prototype were found. Characteristic impedances of this initial approximation are in the range limited by $Z_{\min A}$ = 18.4 Ω and $Z_{\max A}$ = 135.9 Ω, and satisfy condition (1). In the second stage, parameters of the filter were optimized assuming presence of discontinuities. During the optimization process the impedance of the last section attained 50 Ω and a filter having 17 sections was finally obtained. Table II shows the filter parameters after optimization, and its construction is shown in Figure 14.

Figure 15 and Figure 16 show the experimental and theoretical S_{11} and S_{21} curves of the filter. The influence of discontinuities was taken into account in case of theoretical characteristics. It should be pointed out that there is a very good agreement between theoretical and experimental responses in the whole analyzed frequency range. It confirms very high practical value of the method described in this paper. As in the case of Filter I, substantial influence of parasitic modes on the responses of the filter was not observed.

In order to evaluate the influence of discontinuities on the response of the filter, experimental and theoretical characteristics of Filter II were compared (neglecting the influence of discontinuities), see Figure 17.

It was observed that theoretical characteristics obtained in this way are shifted towards greater frequencies. The theoretical stop band of the filter is greater than the same band found experimentally. Degradation of S_{11} curves in the pass band was not observed. It is the result of smaller influence of discontinuities in the pass band of Filter II, which follows from the fact that the characteristic impedance range of Filter II is narrower than the respective range for Filter I. In the case of Filter II, the diameter of the coaxial line outer conductor in the pass band is also smaller with respect to the wavelength λ.

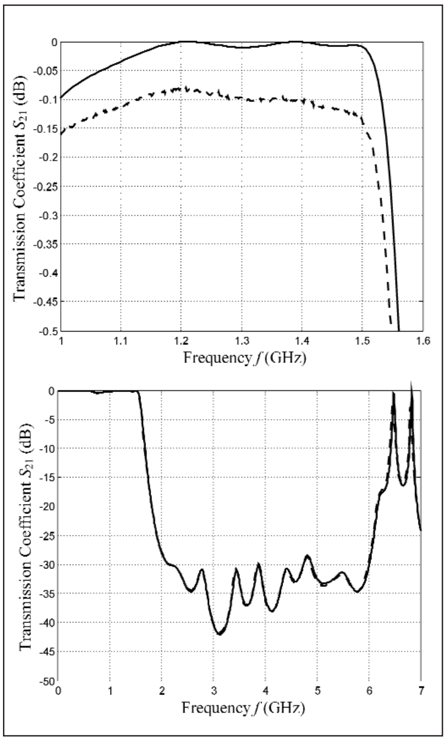

Figure 16 · Theoretical (solid line) and experimental (dashed line) S_{21} responses of Filter II.

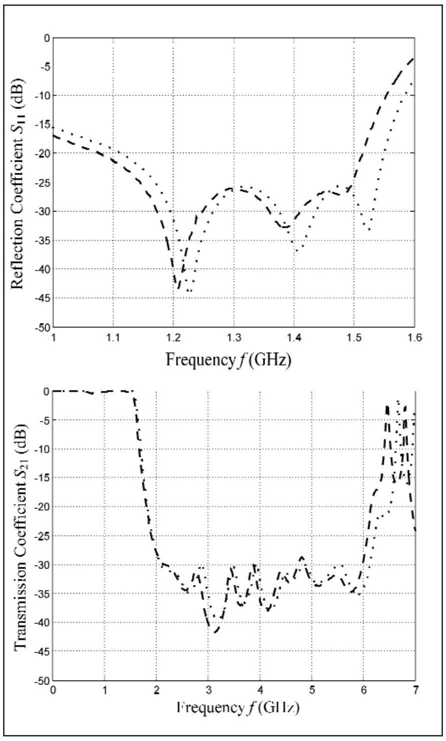

Figure 17 · Comparison of experimental (dashed line) and theoretical (dotted line) S_{11} and S_{21} responses of Filter II obtained assuming the lack of discontinuities.

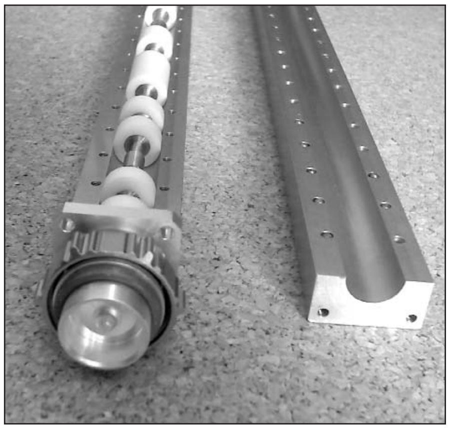

Figure 18 · Construction outline of Filter III.

Making use of the above conclusions it can be assumed that in some cases the filter designed without taking the discontinuities into account can have characteristics satisfying the requirements only after shortening the filter by 1 or 2 percent (equal shortening of each section).

Filter III

The third filter was designed assuming that the pass and stop bands are determined by the following frequencies: f_d = 1.20 GHz, f_1 = 1.45 GHz, f_2 = 2 GHz and f_u = 12 GHz (see Fig. 3). The characteristic impedance range of particular sections was limited by Z_{min} = 25 Ω and Z_{max} = 90 Ω. It was assumed that S_{11} < –23 dB in the pass band and the insertion loss in the stop band should not be less than 20 dB. This filter was implemented using coaxial line technology with the outer diameter equal to 16 mm and terminated in the same manner as Filter II.

Previously, the way to obtain the initial approximation for the optimization process was described. Table III shows parameters of the filter obtained using the optimization procedure, in which the lack of discontinuities was assumed. Construction outline of Filter III is shown in Figure 18.

Figure 19 and Figure 20 show the experimental and theoretical curves of S_{11} and S_{21} of Filter III. Divergence between these curves is small in the low frequency region and is growing with frequency. It is the opinion of the author that the parasitic modes (near the upper limit of the analyzed frequency range) and the growing influence of discontinuities, which were not taken into account during the design stage, are the cause of these divergences. Theoretical stop band of the filter is narrower in comparison with the measured result. As in the case of Filter II, degradation of S_{11} in the pass band was not observed.

Sec. No. i	Component filter sect. No. j	Z_{0i} (Ω)	Inner conduct. diam. d_i (mm)	Diel. const. ε_r	Sec. length l_i (mm)	Sec. length l_i (ε_r=1) (mm)
1	1	46.	5.33	2.03	14.55	20.73
2	2	67.	5.15	1	21.19	21.19
3	3	46.	5.33	2.03	14.84	21.14
4	4	73.	4.68	1	21.07	21.07
5	5	57.	6.18	1	21.13	21.13
6	6	75.	4.52	1	21.02	21.02
7	7	39.	6.30	2.03	14.87	21.19
8	8	82.	4.07	1	21.16	21.16
9	9	39.	6.30	2.03	14.84	21.14
10	10	58.	6.07	1	21.21	21.21
11	11	39.	6.30	2.03	14.80	21.09
12	12	83.	3.95	1	21.18	21.18
13	13	25.	8.80	2.03	14.84	21.14
14	14	88.	3.66	1	21.15	21.15
15	15	37.	8.63	1	21.18	21.18
16	16	25.	8.80	2.03	14.81	21.10
17	17	73.	4.66	1	21.11	21.11
18	18	25.	8.80	2.03	14.91	21.24
19	1	25.	8.80	2.03	7.35	10.47
20	2	25.	8.80	2.03	7.42	10.57
21	3	86.	3.80	1	10.65	10.65
22	4	69.	4.98	1	10.59	10.59
23	5	25.	8.80	2.03	7.37	10.50
24	6	53.	6.51	1	10.09	10.09
25	7	25.	8.80	2.03	7.87	11.21
26	8	87.	3.72	1	10.43	10.43
27	9	51.	6.74	1	10.28	10.28
28	10	86.	3.81	1	11.02	11.02
29	11	30.	7.72	2.03	7.22	10.29
30	12	67.	5.20	1	10.28	10.28
31	13	30.	7.72	2.03	7.80	11.11
32	14	73.	4.66	1	10.25	10.25
				$\sum l_i$ –	458.4	

Table 3 · Electrical and construction parameters of Filter III.

As the design process was, in the case of Filter III, limited mainly to the amplitude synthesis (reducing the characteristic impedances of each

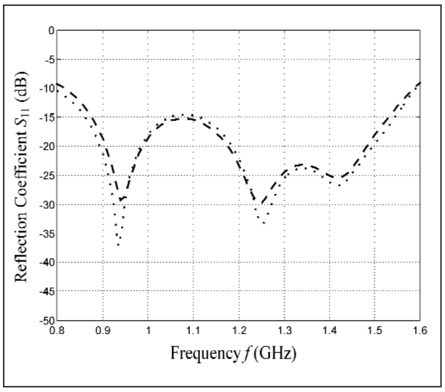

Figure 19 · Theoretical (dashed line) and experimental (dotted line) S_{11} responses of Filter III.

section to the prescribed limits). Table 3, col. 7, shows that the theoretical characteristics of the filter has a periodic form, as confirmed by the measurement in Figure 21.

The group delay of Filter II with a little ripple slightly above the pass band (1.15-1.5 GHz) is presented in Figure 22 as an example of typical group delay for filters under consideration.

Conclusions

In this article, useful method of band-stop filter design has been presented, in which construction constraints, formulated by means of the characteristic impedance range of its particular sections, are taken into account. The insertion loss frequency response of the designed filters is close to the equal-ripple in both the pass- and stop-band.

In order to confirm the usefulness of this method, the three coaxial band-stop filters were designed, manufactured and tested. One of the filters was designed by means of the original spline procedure applied to the insertion loss frequency responses. As it follows from the comparison of theoretical and experimental characteristics, proposed spline procedure makes possible the design of band-stop filters with relatively broad stop bands.

It was also found that there is a very good synchronization between experimental and theoretical responses (determined in presence of discontinuities) in the wide frequency range. The observed divergences are very small and remain constant in function of frequency. In case of neglecting the discontinuities during the design process, theoretical characteristics differ from the experimental as follows:

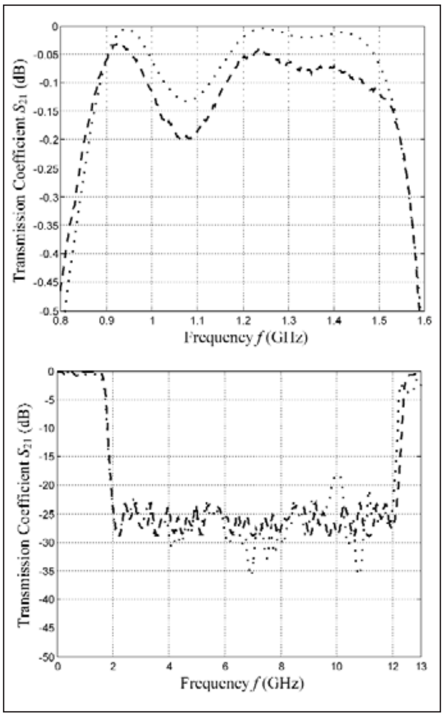

Figure 20 · Theoretical (dashed line) and experimental (dotted line) S_{21} responses of Filter III (theoretical characteristics without the influence of discontinuities).

(a) The real curve is shifted towards lower frequencies, with respect to the theoretical characteristic.
(b) The measured stop band of the filter is narrower than the theoretical one.
(c) In some cases the measured S_{11} characteristic in the pass band is a deformed version of the theoretical one.

All discrepancies mentioned above are proportional to the range of characteristic impedances of particular sections of the filter and to the transversal dimensions of the filter, in relation to the wavelength λ (for example, the diameter of the outer conductor of the coaxial line).

It can be also assumed that in certain cases the filter can be designed without taking into account the influence of discontinuities. In this case it would be recommended to shorten equally each filter section by one or two percent for partial compensation of discontinuities.

All of the analyzed filters introduce a pass-band loss, which was found to be not greater than 0.2 dB. Group delay of all tested filters is nearly constant in the pass band with a little ripple above.

References

1. S. Rosloniec, *Algorithms for computer aided design of linear microwave circuits.* Boston: Artech House, 1990, Ch. 4, 5.

2. S. Rosloniec, "About the application of the stepped transmission lines in linear microwave circuit design" (in Polish). Prace Naukowe PW, Elektronika z. 84 (WPW), Warsaw, Poland, 1990.

3. P. Dyderski, "Algorithms for designing of microwave noncommensurate stepped transmission line band-stop filters" (in Polish). M.S. thesis, The Faculty of Electronics and Information Technology, Warsaw University of Technology, Warsaw, Poland, 1999.

4. S. Rosloniec, "Application of the R-transformer to the Design of Microwave Harmonic Filters." *Archiv fur Elektronic und Ubertragungstechnik* (Electronics and Communication), AEU - Band 41, Heft 4, pp. 251-253, 1987.

5. N. Riblet, "General synthesis of quarter-wave impedance transformers." *IRE Trans. Microwave Theory and Tech.,* Vol. MTT 5, pp. 36-43, Jan. 1957.

6. C. G. Montgomery, R. H. Dicke,

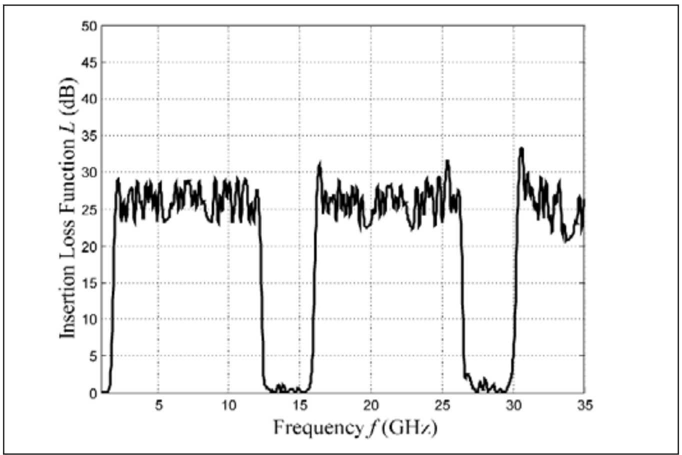

Figure 21 · Illustration of periodicity of the stop bands of Filter III being a cascade of two filters (theoretical characteristics without the influence of discontinuities).

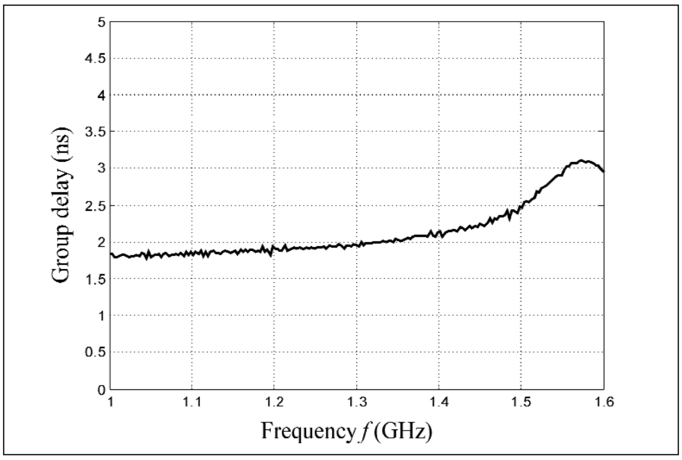

Figure 22 · Group delay for Filter II. This behavior is typical for the type of filters examined.

and E. M. Purcell, *Principles of microwave circuits (*2nd ed.). London/UK: Peter Peregrinus Ltd., 1987, Ch. 4.

7. B. C. Wadell, *Transmission line handbook.* Boston: Artech House, 1991.

8. V. F. Demianov and V. N. Malozemov, *Introduction to minimax.* New York: Wiley, 1974.

9. B. N. Pshenichnyj, *The linearization method for constrained optimization.* Berlin: Springer-Verlag, 1994.

10. P. Dyderski, "Noncommesurate, stepped transmission line band-stop filters" (in Polish). *Proceedings of the Telecommunications Research Institute,* No. 124, pp. 10-17, Warsaw, Poland, 1999.

11. N. Marcuvitz (ed.), *Waveguide handbook* (2nd ed.). London/UK: Peter Peregrinus Ltd., 1986, pp. 310-312.

12. M.A.R. Gunston, "A Simple Formula for Calculating Approximate Values of the First Zeros of a Combination Bessel Function Equation." *IEEE Trans. Microwave Theory and Tech.,* Vol. MTT 11, pp. 93-94, Jan. 1963.

13. J. A. Cochran, "Further Formulas for Calculating Approximate Values of the Zeros of Certain Combinations of Bessel Functions." *IEEE Trans. Microwave Theory and Tech.,* Vol. MTT 11, pp. 546-547, Nov. 1963.

14. G. Matthaei, L. Young, and E.M.T. Jones, *Microwave filters, impedance-matching networks, and coupling structures.* New York: McGraw-Hill Inc., 1964, Ch. 6, 8.

15. S. Rosloniec, Faculty of Electronic, Warsaw University of Technology, Warsaw, Poland, private communication.

Author Information

Piotr Dyderski was born in Przysucha, Poland, on June 22, 1974. He received his M.S. degree in electronic engineering from Warsaw University of Technology, Warsaw, Poland, in 1999. Since 1998 he has been involved with Passive Microwave Devices Dept. of the Telecommunications Research Institute, Warsaw, Poland. His current research interests include computer-aided design of equiphase array antennas and microwave circuits, especially filters and rotary joints for radiolocations and radionavigations systems. He can be reached by e-mail at: Piotr.Dyderski@pit.edu.pl.